Intrathecal transplantation of human umbilical cord mesenchymal stem cells enhances spinal cord injury recovery: Role of miR-124-3p as a biomarker

YITONG ZHENG*, YONGXIN WANG*, WEN LIU*, MUJITE A, YABIN LI, XIAOHU MA, MIERADILI ABULIMITI, NUERAILIJIANG MAIMAITIAILI and HU QIN

Department of Neurosurgery, The First Affiliated Hospital of Xinjiang Medical University, Urumqi, Xinjiang Uygur Autonomous Region 830000, P.R. China

Received September 8, 2024; Accepted December 18, 2024

DOI: 10.3892/etm.2025.12807

Abstract. Spinal cord injury (SCI) is a severe condition that often leads to permanent functional impairments. The current treatment options are limited and there is a need for more effective treatments. Human umbilical cord mesenchymal stem cells (hUCMSCs) have shown promise in promoting neuroregeneration and modulating immune response. In addition, miR-124-3p has been identified as a potential biomarker for monitoring the progress of neural repair, making it a focus of the present study, which used a rat model of SCI to evaluate the effects of intrathecal hUCMSC transplantation. The present study included three groups: A sham-operated group, an SCI model group receiving PBS and an SCI group receiving hUCMSCs. Neurological function was assessed using the Basso, Beattie and Bresnahan locomotor rating scale and Rivlin inclined plane test on days 1, 3, 7, 14 and 21 post-injury. Histological analysis included hematoxylin and eosin staining to assess tissue morphology, Nissl staining to evaluate neuron survival and immunofluorescence to detect bromodeoxyuridine (BrdU)+/neuron-specific enolase (NSE)+ cells, which indicate neurogenesis. Detection of brain-derived neurotrophic factor (BDNF) protein expression at various time points in rats with spinal cord injury using western blotting. miR-124-3p expression was quantified using reverse transcription-quantitative (RT-q)PCR to assess its potential as a biomarker for SCI recovery. The hUCMSC group showed significant improvements in motor function compared with the control group, particularly on days 7 and 14 post-injury. Histological analysis revealed reduced scar tissue formation and increased neuron survival in the hUCMSC group. Immunofluorescence analysis showed a higher number of BrdU+/NSE+ cells in the hUCMSC group, indicating enhanced neurogenesis. The expression of the neurorepair-related protein BDNF was markedly higher in the hUCMSCs group compared with the control group. Furthermore, RT-qPCR analysis demonstrated a marked upregulation of miR-124-3p in the hUCMSC group, which was correlated with improved functional recovery. The present study demonstrated that intrathecal transplantation of hUCMSCs notably enhanced recovery following SCI, probably by promoting neurogenesis and modulating miR-124-3p expression. miR-124-3p upregulation in the hUCMSC group highlighted its potential as a biomarker for tracking the progress of SCI recovery. These findings provided a foundation for the future clinical applications of hUCMSCs in SCI treatment and the use of miR-124-3p as a monitoring tool.

Introduction

Spinal cord injury (SCI) is a severe central nervous system injury typically caused by external trauma, such as car accidents, falls or sports activities (1). This type of injury can lead to partial or complete destruction of the spinal cord, resulting in a series of complex pathophysiological changes, including primary and secondary injuries. Primary injury is usually due to the direct mechanical force acting on the spinal cord, such as vertebral fractures, dislocations or ligament tears, leading to compression, contusion or complete transection of the spinal cord. Secondary injury refers to the series of biological reactions that occur following primary injury, including neuroinflammation, disruption of the blood-brain barrier, oxidative stress, apoptosis and demyelination (2). These secondary responses further exacerbate neuronal damage, leading to extensive neurological dysfunction and markedly increase the difficulty of SCI patient rehabilitation. Current treatment strategies for SCI mainly focus on surgical intervention and pharmacological therapy in the acute phase, aiming to mitigate secondary injury and promote nerve regeneration (3).

Correspondence to: Professor Hu Qin, Department of Neurosurgery, The First Affiliated Hospital of Xinjiang Medical University, 137 Liyuushan South Road, Urumqi, Xinjiang Uygur Autonomous Region 830000, P.R. China
E-mail: qinhu86@163.com

*Contributed equally

Key words: spinal cord injury, human umbilical cord mesenchymal stem cells, neurogenesis, miR-124-3p, biomarker, stem cell therapy, intrathecal transplantation, functional recovery

However, these conventional treatments have limited efficacy in restoring neurological function and are unable to reverse the long-term disabilities caused by the injury. Therefore, developing more effective therapies to promote nerve regeneration and functional recovery has become a focal point of SCI research.

In recent years, with the rapid development of stem cell technology, the application of stem cell therapy in SCI treatment has gained widespread attention. Stem cells, particularly mesenchymal stem cells (MSCs), have emerged as a potential treatment option for SCI due to their multilineage differentiation potential, low immunogenicity and immunoregulatory abilities (4). Among the various sources of MSCs, human umbilical cord MSCs (hUCMSCs) have become a research focus due to their easy accessibility, minimal ethical concerns and excellent differentiation and proliferation potential. hUCMSCs can differentiate into multiple types of neural cells, such as neurons and astrocytes and an also modulate the microenvironment of the injury site by secreting bioactive molecules, thereby suppressing inflammatory responses and promoting nerve regeneration (5,6). Specifically, the mechanisms through which hUCMSCs contribute to SCI repair include the following: First, hUCMSCs can secrete various cytokines and growth factors, such as brain-derived neurotrophic factor (BDNF) and nerve growth factor, to directly promote neuronal survival and regeneration (7,8). Second, hUCMSCs can modulate the inflammatory response at the injury site, inhibiting the activation of inflammatory cells and reducing further damage to neurons from secondary injury. In addition, hUCMSCs can secrete exosomes and microRNAs (miRNAs), such as miR-124-3p, which regulate neuronal differentiation and axon growth, playing a significant role in neural repair (9,10).

miR-124-3p is an miRNA highly expressed in the nervous system, considered to play a crucial role in neuronal differentiation and functional maintenance (11). Studies have shown that miR-124-3p is markedly upregulated following nerve injury, promoting neuronal regeneration and axonal repair by targeting multiple signaling pathways (12,13). For example, PPG alleviates ischemia-induced neuronal injury and microglial inflammation by regulating the miR-124-3p/tumor necrosis factor receptor-associated factor 6/NF-κB pathway (13). Furthermore, miR-124-3p has been found to regulate neuroinflammatory responses by modulating macrophage polarization, thereby reducing the release of inflammatory factors and mitigating secondary inflammatory responses following neural injury (14). In the context of SCI repair, the role of miR-124-3p is attracting attention and is regarded as a potential biomarker. Changes in its expression level can reflect the progress of neural repair and provide a new method for monitoring clinical treatment efficacy. Studies have indicated that miR-124-3p upregulation is closely associated with neurological recovery, highlighting its promising application prospects in SCI treatment (15). Despite the emerging understanding of the mechanisms through which hUCMSCs and miR-124-3p contribute to SCI repair, challenges remain. For instance, the heterogeneity of hUCMSCs may lead to inconsistent therapeutic outcomes. In addition, although the role of miR-124-3p in SCI repair has been partially validated, its complex mechanism of action requires further elucidation.

In conclusion, the combined application of hUCMSCs and miR-124-3p offers new hope for SCI treatment. The in-depth exploration of this research direction will not only help improve SCI treatment outcomes but also lay the theoretical foundation for future clinical applications. As research progresses, hUCMSCs and miR-124-3p are expected to become key tools in SCI treatment, providing patients with improved rehabilitation opportunities and improved quality of life.

Materials and methods

Ethical statement. All animal experiments were approved by the Animal Ethics Committee of the Xinjiang Medical University (Urumqi, China; approval no. IACUC-20230321-07). All procedures involving animals complied with the principles of laboratory animal management and protection (16), with measures taken to minimize the number of animals used and their suffering.

The study adhered to the Animal Research: Reporting of *In Vivo* Experiments (ARRIVE) guidelines to ensure transparency and reproducibility. Humane endpoints were established and animals were sacrificed if they exhibited severe pain, sustained weight loss exceeding 15%, or significant loss of mobility. The total duration of the experiment was 35 days, from the establishment of the model to the final data collection. A total of 36 healthy 8-week-old female specific pathogen-free-grade Sprague-Dawley rats weighing 220-250 g were purchased from the Animal Experiment Center of Xinjiang Medical University (Urumqi, China), all of which successfully completed the study without any mortality. Animal health and behavior were monitored twice daily (morning and afternoon), focusing on body weight, mobility, dietary intake, hydration and wound recovery. To minimize suffering and distress, all surgical procedures were performed under anesthesia with 1% sodium pentobarbital (40 mg/kg). Animals were housed in individualized cages maintained under controlled conditions, including a temperature of 22±2˚C, a relative humidity of 50-60% and a 12-h light/dark cycle. They were provided with free access to soft food and adequate hydration. Mortality was confirmed through the absence of spontaneous respiration, fixed and dilated pupils, cessation of heartbeat and lack of reflex activity.

hUCMSCs. The hUCMSCs used in the present study were purchased from Xinjiang Western Saiou Biotechnology Co., Ltd. (cat. no. WC-2023128). The hUCMSCs used in the experiments were at passages 3-5 and underwent standardized cultivation and quality control by the company to ensure their multilineage differentiation potential and the expression of typical mesenchymal stem cell surface markers.

Characterization of hUCMSCs. The characterization of hUCMSCs included the following processes.

Surface marker detection. The surface markers of hUCMSCs were analyzed by flow cytometry. Cells were washed with PBS, digested with trypsin and collected by centrifugation (300 x g; 5 min; 4˚C). A total of $1x10^6$ cells were suspended in 100 μl PBS and corresponding FITC- or PE-conjugated antibodies were added, including anti-CD73, anti-CD90 and

Figure 1. Neuroendoscopic-assisted modeling. (A) Neuroendoscope, (B) spinal cord under direct visualization and (C) neuroendoscopic view of the spinal cord.

anti-CD105 for positive markers and anti-CD34, anti-CD45 and anti-HLA-DR as negative controls (BD Biosciences). Following mixing, the cells were incubated in the dark for 30 min at 4˚C, washed twice with PBS and analyzed using a flow cytometer (FACSCalibur; BD Biosciences). The results were processed using FlowJo software (version 10.10; FlowJo LLC).

Osteogenic differentiation. Passage 3 hUCMSCs were seeded in a 6-well plate and when the cells reached ~70% confluence, they were cultured in osteogenic induction medium (containing 100 nM dexamethasone, 10 mM β-glycerophosphate and 50 μg/ml ascorbic acid). After 21 days, the cells were fixed with 4% paraformaldehyde for 15 min at room temperature, stained with Alizarin Red for 30 min at room temperature and observed under a light microscope (Olympus Corporation) at x400 magnification. Three random fields were examined to assess osteogenic nodules, with fields selected to avoid overlaps.

Chondrogenic differentiation. Cells were suspended in chondrogenic induction medium containing 10 ng/ml TGF-β3 and cultured at 37˚C in a 5% CO_2 incubator for 3 weeks. The cartilage matrix was observed using Alcian Blue staining, performed for 30 min at room temperature.

Adipogenic differentiation. Cells were seeded in a 6-well plate and cultured in adipogenic induction medium (containing 1 μM dexamethasone, 10 μg/ml insulin, 0.5 mM isobutylmethylxanthine and 200 μM indomethacin) at 37˚C in a 5% CO_2 incubator for 14 days. After fixation with 4% paraformaldehyde for 15 min at room temperature, the cells were stained with Oil Red O for 30 min at room temperature and lipid droplets were observed under a light microscope (Olympus Corporation) at x400 magnification. Three fields were randomly selected to avoid overlapping regions.

Rat spinal cord injury model. SD rats were selected due to their anatomical and physiological similarity to humans, making them a widely accepted model for SCI studies. Female rats were used to ensure consistent hormonal levels and reduced variability in experimental outcomes compared to males. Additionally, their physiological structure facilitates easier assistance with urination after SCI model establishment, which is critical for postoperative care. An improved Allen method (17) was used to establish the SCI model and the entire procedure was performed under neuroendoscopy (Fig. 1). First, the rats were anesthetized with 1% sodium pentobarbital (40 mg/kg) via intraperitoneal injection and placed in a prone position with T9-T11 as the surgical range and T10 as the center. The surgical area was shaved and disinfected with iodine. A 2.5 cm longitudinal skin incision was made and subcutaneous fat and fascia were bluntly dissected. The surgical knife was used to sharply dissect along the spinous processes, retracting the muscles on both sides and the supraspinous and interspinous ligaments of T9-T11 were cut to fully expose the spinous processes and lamina of T9-T10. A mosquito hemostat was used to gently lift the T10 spinous process and an ophthalmic scissor was used to carefully cut open the lamina on both sides of the T10, lifting the posterior wall of the vertebral canal, with partial removal of the lateral walls to fully expose the T10 spinal segment. A small elliptical iron plate (~5 mm^2 in area and 1 mm in thickness) was then placed over the T10 segment and a 20 g Kirschner wire was dropped freely from a height of 3.5 cm using a modified 1 ml syringe sleeve to strike the T10 spinal segment. Following the strike, significant congestion and edema were observed at the corresponding site, with transient tail flicks and sustained hindlimb spasms and tremors in the rats. Finally, the surgical area was irrigated with sterile saline and the incision was closed layer by layer.

The experimental animals were randomly divided into three groups: Sham-operated, model and hUCMSC groups, with 12 rats in each group. In the sham-operated group, the spinal cord was exposed and the incision was immediately closed. In the model group, the SCI model was established after exposing the spinal cord, followed by an intrathecal injection of 20 μl PBS. In the hUCMSC group, the SCI model was similarly established, followed by an intrathecal injection of 20 μl hUCMSCs under neuroendoscopy.

Evaluation of hindlimb motor function in rats. On days 1, 3, 7, 14 and 21 post-SCI, hindlimb motor function in rats was assessed using the Basso, Beattie and Bresnahan (BBB) score and the Rivlin inclined plate tests (18,19). The BBB score comprehensively evaluates hindlimb function in terms of early joint movement, mid-stage gait and coordinated movement and fine paw movement during locomotion. The scoring range was 0-21, with 0 indicating complete paralysis and 21 indicating normal hindlimb function. This method was used to evaluate the recovery of hindlimb function. The Rivlin inclined plate test involved placing rats on a flat inclined plate made of a 1-cm thick wooden board with a 0.5-cm thick rubber pad. The inclined plate was gradually tilted from 0˚ at 5˚ increments and the maximum angle at which the rat could remain on the plate without slipping for 5 sec was recorded using a protractor. All functional assessments were independently completed by two blinded researchers, with each rat being evaluated three times

Table I. Sequence of each gene and internal reference primer.

Name of primer	Primer Sequences (5'-3')
U6 forward	CTCGCTTCGGCAGCACA
U6 reverse	AACGCTTCACGAATTTGCGT
rno-miR-124-3p-RT	CTCAACTGGTGTCGTGGAGTCGGCAATTCAGTTGAGGGCATTCA
rno-miR-124-3p forward	ACACTCCAGCTGGGTAAGGCACGCGGTG
Universal reverse	TGGTGTCGTGGAGTCG

miR, microRNA.

and the average value was taken as the final result to ensure data accuracy and reliability.

Sample collection. Hindlimb motor function was evaluated on days 1, 3, 7, 14 and 21 and three rats were randomly selected at each time point. Following intraperitoneal overdose anesthesia with 1% pentobarbital sodium (80 mg/kg), the rats were sacrificed by cervical dislocation and the chest was opened to expose the ascending aorta and heart. Each rat was perfused with 0.9% saline to remove circulating blood and the spinal cord tissue from the injury site (0.5-1 cm) was collected on ice for pathological examination and reverse transcription-quantitative (RT-q) PCR. Samples for pathological examination were fixed in 4% paraformaldehyde at 4˚C for 24 h, dehydrated in an ethanol gradient (70, 80, 90, 95 and 100% ethanol, for 1 h each), cleared in xylene (10 min twice) and embedded in paraffin at 60˚C for 2 h. The tissues were sectioned into 5-μm thick spinal cord rings for hematoxylin and eosin (H&E) staining, Nissl staining and immunofluorescence. Samples for RT-qPCR were preserved in RNA stabilization solution for subsequent miRNA extraction and analysis. Samples for western blotting were stored at -80˚C.

H&E and Nissl staining. The embedded rat spinal cord tissue was sectioned and fixed in 4% paraformaldehyde at 4˚C for 24 h. Paraffin-embedded sections were deparaffinized with environmentally friendly deparaffinization solution, dehydrated in an ethanol gradient and washed with distilled water. H&E staining was performed at room temperature for 5 min in hematoxylin and 2 min in eosin, followed by dehydration and clearing. Following drying, histological and morphological changes were observed under a light microscope (Leica Microsystems GmbH). For Nissl staining, suitable spinal cord sections were selected, washed with PBS, placed on slides, stained with Nissl staining solution for 20 min at room temperature, dehydrated, cleared and mounted for observation under a light microscope (Leica Microsystems GmbH) at x200 magnification. Three fields were randomly selected to avoid overlapping regions.

Bromodeoxyuridine (BrdU) labeling. Each group of rats was intraperitoneally injected with BrdU saline solution (10 mg/100 g) twice daily (at 8-h intervals) on days 1, 2, 5, 6, 12, 13, 19 and 20 before sacrifice.

Immunofluorescence staining. Spinal cord tissues fixed in 4% paraformaldehyde at 4˚C for 24 h were embedded in paraffin. The tissue was dehydrated in an ethanol gradient (70, 80, 90, 95 and 100%, for 1 h each), cleared in xylene (10 min twice) and embedded in paraffin at 60˚C for 2 h. Paraffin blocks were sectioned into 10-μm thick slices. Sections were treated with 0.5% Triton X-100 for 20 min, followed by 0.6% H_2O_2 for 15 min to remove endogenous peroxidase activity. A drop of 10% normal goat serum (Gibco; Thermo Fisher Scientific, Inc.) was applied and the sections were incubated at 37˚C for 30 min to block nonspecific binding. Primary antibodies were then added: Anti-BrdU antibody (mouse origin; dilution, 1:200; Sigma-Aldrich; Merck KGaA; cat. no. B8434) and anti-neuron-specific enolase (NSE) antibody (mouse origin; dilution, 1:50; Abcam; cat. no. ab180943) and incubated overnight at 4˚C. The next day, sections were washed three times with PBS for 5 min each and secondary antibodies were added: Anti-mouse Cy3-conjugated secondary antibody (dilution, 1:500; Abcam; cat. no. ab97035) for BrdU-positive cell detection and anti-mouse FITC-conjugated secondary antibody (dilution, 1:1,000; Abcam; cat. no. ab6785) for NSE-positive cell detection, followed by incubation at 37˚C for 30 min. DAPI staining (dilution, 1:1,000; 10 min at room temperature; Abcam; cat. no. ab228549) was used to label cell nuclei. Following washing with PBS, the sections were observed and imaged under a fluorescence microscope (Olympus Corporation) to analyze the number of BrdU and NSE double-positive cells.

RT-qPCR. Total RNA was extracted from spinal cord tissue using TRIzol® reagent (Thermo Fisher Scientific, Inc.), according to the manufacturer's instructions and RNA concentration and purity (A260/A280) were measured using a NanoDrop 2000 spectrophotometer (NanoDrop Technologies; Thermo Fisher Scientific, Inc.). RNA (1 μg) was reverse transcribed into cDNA using the PrimeScript RT Reagent Kit (Takara Bio, Inc.). The RT reaction conditions were 37˚C for 15 min, 85˚C for 5 sec and holding at 4˚C. RT-qPCR was performed using SYBR Green PCR Master Mix (Takara Bio, Inc.) on a 7500 Fast Real-Time PCR System (Thermo Fisher Scientific, Inc.). Each reaction mixture contained a total volume of 20 μl, including 10 μl SYBR Green mix, 0.4 μM forward primer, 0.4 μM reverse primer, 2 μl cDNA template and nuclease-free water up to 20 μl. Primer sequences are shown in Table I. All RT-qPCR experiments were repeated three times and the relative expression level of miR-124-3p was calculated using the $2^{-\Delta\Delta Cq}$ method (20), with U6 as the internal control.

Western blotting. To analyze BDNF protein expression, total protein was extracted from the rat spinal cord injury site using RIPA lysis buffer (Beijing Solarbio Science & Technology Co., Ltd.) and concentrations were measured with a BCA assay (Thermo Fisher Scientific, Inc.; cat. no. 23225). Equal amounts (30 μg) of protein were separated on 10% SDS-PAGE gels and transferred onto PVDF membranes (MilliporeSigma; cat. no. IPVH00010). Membranes were blocked with 5% non-fat milk in TBST (0.1% Tween-20) at room temperature for 1 h, then incubated overnight at 4˚C with anti-BDNF primary antibody (1:1,000, Abcam; cat. no. ab108319). After three washes, the membranes were incubated with an HRP-conjugated secondary antibody (1:10,000, Abcam; cat. no. ab6721) for 1 h at room temperature. Protein bands were detected with ECL (Thermo Fisher Scientific, 34580) and quantified using ImageJ software (version 1.53; National Institutes of Health), normalized to GAPDH (1:10,000, Abcam; cat. no. ab181602) expression.

Statistical analysis. All data analyses were performed using SPSS 21.0 (IBM Corp.) and GraphPad 7.0 software (Dotmatics). Measurement data were expressed as the mean ± standard deviation. Differences between two unpaired groups with normal distribution and homogeneous variance were analyzed using an unpaired t-test, while differences among multiple groups were analyzed using one-way ANOVA. Post hoc multiple comparisons were performed using Tukey's HSD test when significant differences were observed. $P<0.05$ was considered to indicate a statistically significant difference.

Results

Identification of hUCMSCs. At passage 3, the isolated cells were analyzed for surface marker expression using flow cytometry. The results showed that the positive rates for CD73, CD105 and CD90 were 98.44, 99.32 and 98.97%, respectively, while those for CD11b, CD45, CD34, CD19 and human leukocyte antigen (HLA)-DR were 1.28, 0.67, 0.75, 0.66 and 0.52%, respectively. These results confirmed that most of the isolated cells were hUCMSCs (Fig. 2A). Subsequently, osteogenic, adipogenic and chondrogenic differentiation experiments were performed on these hUCMSCs. The results showed that these cells exhibited a good differentiation ability under different conditions, successfully differentiating into osteocytes (Fig. 2B), chondrocytes (Fig. 2C) and adipocytes (Fig. 2D), further confirming that we successfully isolated hUCMSCs with multilineage differentiation potential.

Evaluation of hindlimb motor function in rats. The BBB scores of all rats were 21 before surgery, indicating normal hindlimb motor function. On days 1, 3 and 21 post-SCI, there were no significant differences in BBB scores between the control and the hUCMSC groups ($P>0.05$). However, on days 7 and 14 post-surgery, the BBB scores in the hUCMSC group were significantly higher compared with those in the control group ($P<0.05$; Fig. 3A). This indicated that intrathecal transplantation of umbilical cord mesenchymal stem cells had a significant promoting effect on hindlimb motor function recovery at these time points. Similarly, the results of the Rivlin inclined plate test showed that all groups of rats had an angle of 55˚ before surgery, indicating normal hindlimb motor function. On days 1, 3 and 21 post-SCI, there were no significant differences between the control and hUCMSC groups in the Rivlin inclined plate test ($P>0.05$). However, on days 7 and 14 post-surgery, the results in the hUCMSC group were significantly improved compared with those in the control group, with statistically significant differences ($P<0.05$; Fig. 3B).

H&E and Nissl staining. H&E and Nissl staining were performed on day 7 post-SCI to observe the histological changes during the significant improvement of hindlimb motor function. The H&E staining results showed no obvious scar tissue or cavitation structures in the spinal cord tissue of the sham-operated group, with numerous intact neurons observed. By contrast, the control group showed substantial scar tissue and vacuolar necrotic regions. In the hUCMSC group, the number of neurons was markedly higher than in the control group and the vacuolar necrotic regions were notably reduced, indicating a favorable therapeutic effect (Fig. 4A). Nissl staining results further supported these observations. The sham-operated group displayed numerous normally distributed neurons, while the control group showed severe neuronal damage and widespread cavitation. In comparison, the hUCMSC group showed neuronal distribution intermediate between the sham-operated and control groups, suggesting that hUCMSCs promoted neuronal repair to a certain extent (Fig. 4B).

BrdU+/NSE+ expression in spinal cord tissue from rats. Representative images were selected for display on day 7 post-SCI (Fig. 5). Immunofluorescence results showed that the number of $BrdU^+/NSE^+$ double-positive cells in the sham-operated group was significantly lower than that in the other two groups, while the number of $BrdU^+/NSE^+$ double-positive cells in the hUCMSC group was significantly higher than that in the control group ($P<0.05$). These results suggested that more proliferating cells differentiated into neurons following an intrathecal injection of hUCMSCs, or that hUCMSCs may enhance neurogenesis and repair by promoting neuronal proliferation.

BDNF protein expression in rat spinal cord tissue following hUCMSCs transplantation. Western blotting was used to analyze the expression of neurorepair-related proteins in the control and hUCMSC groups in the SCI rat model, specifically investigating the changes in BDNF protein expression at different time points following the intrathecal transplantation of hUCMSCs. The results showed that BDNF expression in the spinal cord tissue of the hUCMSC group was significantly increased compared with the control group on days 7 and 14 ($P<0.05$; Fig. 6).

Comparison of miR-124 expression in spinal cord tissue among the three groups. In the present study, RT-qPCR was used to analyze the expression levels of miR-124-3p in spinal cord tissue in each experimental group, with U6 as an internal reference gene for normalization. The results showed that miR-124-3p expression in the hUCMSC group was significantly decreased on days 7, 14 and 21 post-SCI, as compared with the control group ($P<0.05$) and over time, the rate of increase in miR-124-3p expression in the hUCMSC group was

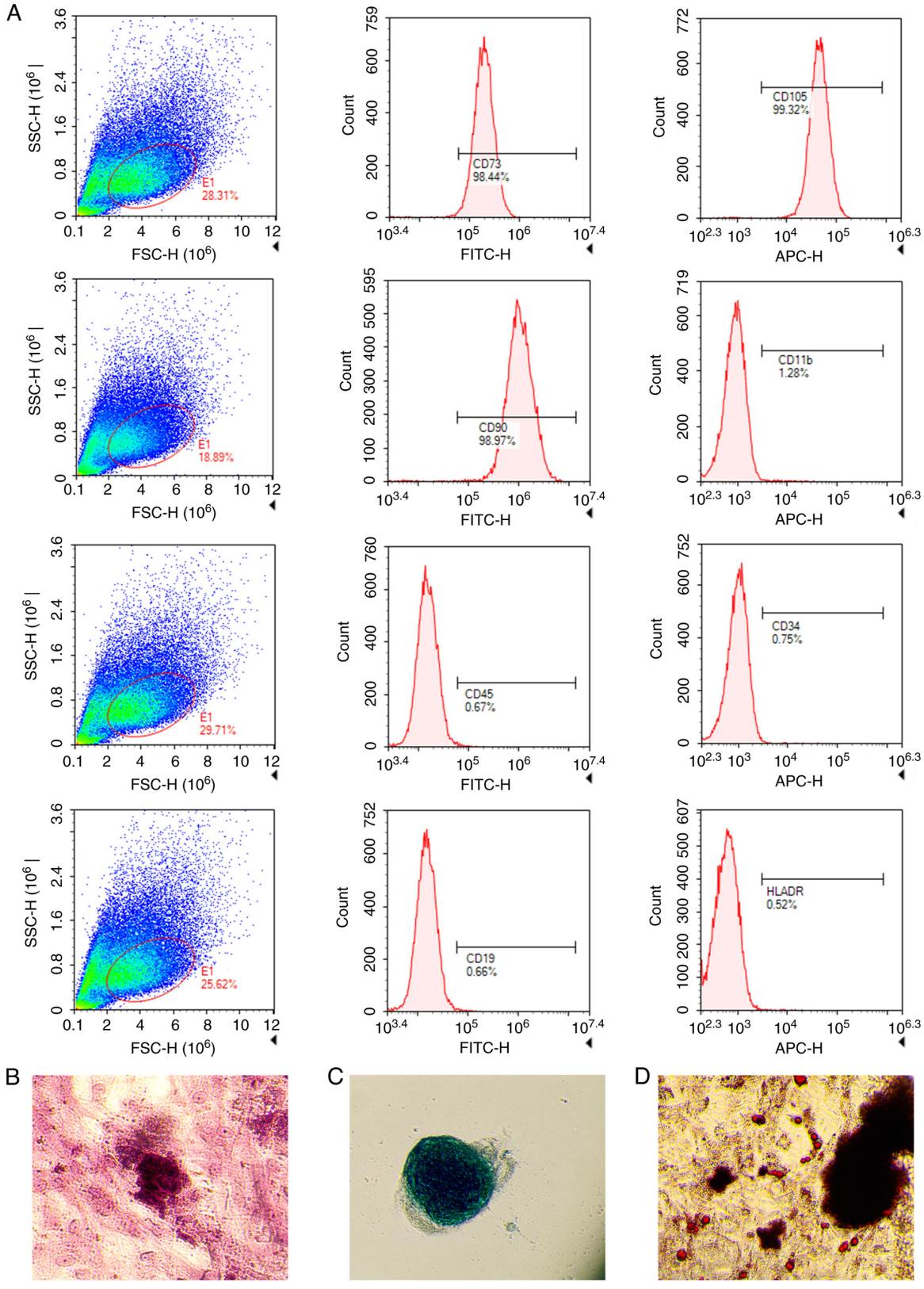

Figure 2. Characterization of human umbilical cord mesenchymal stem cells. (A) Flow cytometry assay. (B) Osteogenic differentiation. (C) Chondrogenic differentiation. (D) Lipogenic differentiation. Magnification, x400.

markedly lower than that in the control group compared to day 3. The sham-operated group showed no significant changes in miR-124-3p expression, with stable expression levels (Fig. 7). These data indicated that miR-124-3p expression is closely associated with the repair process following spinal cord injury, particularly in neural repair following hUCMSCs transplantation, where miR-124-3p showed a significant reduction in upregulation.

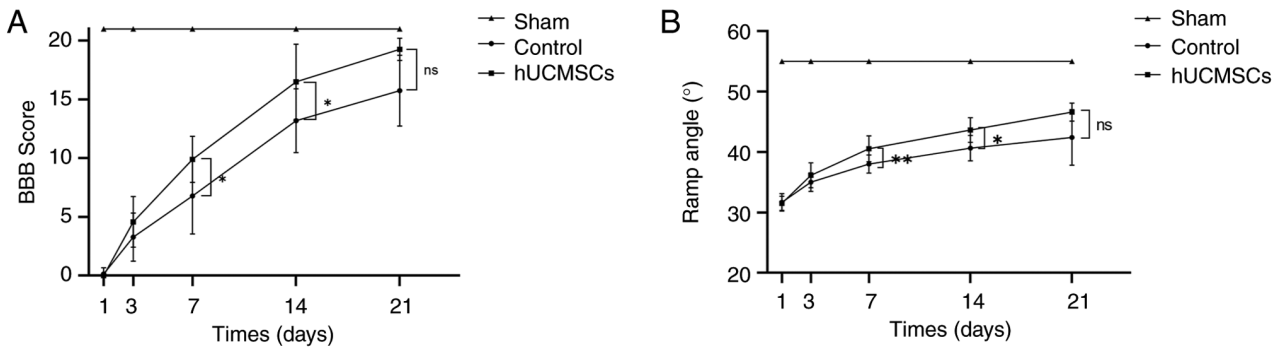

Figure 3. BBB score and Rivlin slant plate test. (A) BBB scores: On postoperative days 7 and 14, the scores in the hUCMSCs group were significantly higher than those in the Control group ($P<0.05$). (B) Rivlin slant plate test: On postoperative days 7 and 14, the results in the hUCMSCs group were significantly improved compared with those in the Control group ($^{*}P<0.05$, $^{**}P<0.01$). BBB, Basso, Beattie and Bresnahan; hUCMSCs, human umbilical cord mesenchymal stem cells.

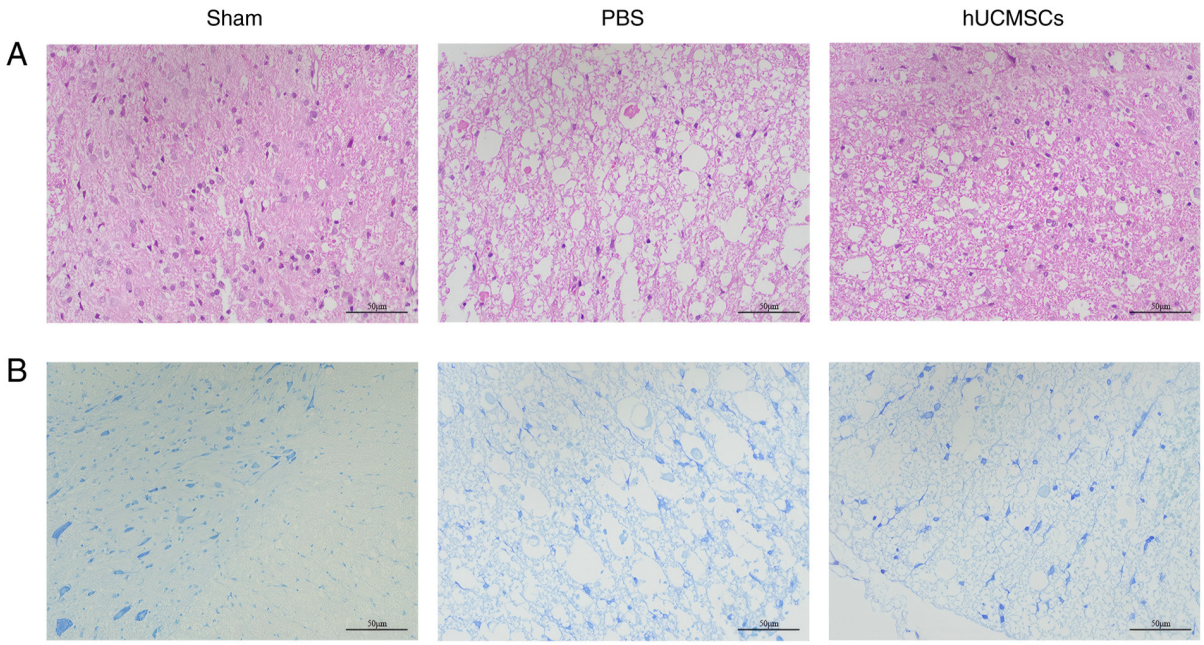

Figure 4. Hematoxylin-eosin and Nissl staining (x200 magnification). (A) Hematoxylin-eosin staining: A large number of intact neuronal cells were observed in the spinal cord tissue of the sham-operated group, while substantial scar tissue and vacuolar necrotic regions were seen in the control group. The vacuolar necrotic regions in the hUCMSCs group were significantly reduced compared to the control group. (B) Nissl staining: The sham-operated group showed a large number of normally distributed neurons, while the control group exhibited severe neuronal damage and widespread cavitation. The neuronal distribution in the hUCMSCs group was intermediate between the sham-operated and control groups. hUCMSCs, human umbilical cord mesenchymal stem cells.

Discussion

Spinal cord injury (SCI) is a severe disease of the CNS that often results in permanent loss of neurological function (1). However, the current pharmacological and non-pharmacological treatment options have limited efficacy in promoting spinal cord repair. Therefore, developing more effective therapeutic strategies is a major focus of scientific research. In recent years, cell transplantation therapies, particularly stem cell-based treatments, have been regarded as promising approaches for treating SCI. hUCMSCs are ideal candidate cells for treating SCI due to their multidirectional differentiation potential, immunoregulatory capabilities and low immunogenicity (21). Studies have shown that hUCMSCs can target damaged tissues, differentiate into functional cells, or secrete immunomodulatory factors, thereby exerting significant therapeutic effects *in vivo* (22). During the repair of SCI, specific biomarkers can serve as effective indicators for monitoring the repair process (23). Among them, miR-124-3p has attracted considerable attention due to its regulatory role in the nervous system, particularly in neuroregeneration. The aim of the present study was to investigate the changes in miR-124-3p expression following intrathecal transplantation of hUCMSCs in SCI repair and evaluate its potential as a monitoring marker for SCI repair.

The main findings of the present study indicated that intrathecal transplantation of hUCMSCs hag a significant therapeutic effect on SCI repair, especially in promoting neuronal proliferation and neuroregeneration. Specifically, immunofluorescence of rat spinal cord tissue post-transplantation revealed

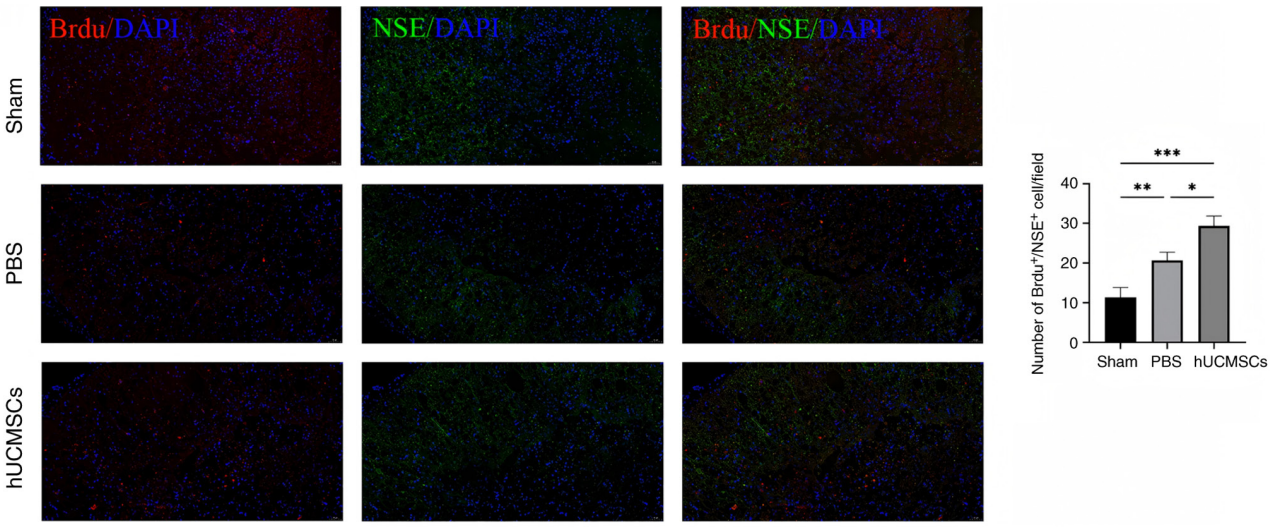

Figure 5. BrdU$^+$/NSE$^+$ expression in rat spinal cord tissues of each group (x200 magnification). The number of BrdU$^+$/NSE$^+$ double-positive cells in the sham-operated group was significantly lower than in the other two groups, while the number of BrdU$^+$/NSE$^+$ double-positive cells in the hUCMSCs group was significantly higher than in the control group (*P<0.05, **P<0.01, ***P<0.001). BrdU, bromodeoxyuridine; NSE, neuron-specific enolase; hUCMSCs, human umbilical cord mesenchymal stem cells.

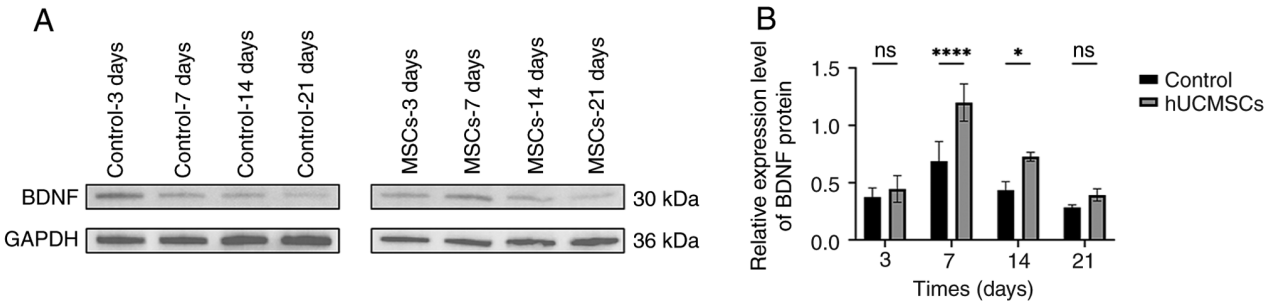

Figure 6. Expression of BDNF protein at various time points in spinal cord injured rats. (A) BDNF protein expression in the control and treatment groups (B) Relative expression statistics of BDNF proteins. BDNF, brain-derived neurotrophic factor. ns, not significant. *P<0.05, ****P<0.0001.

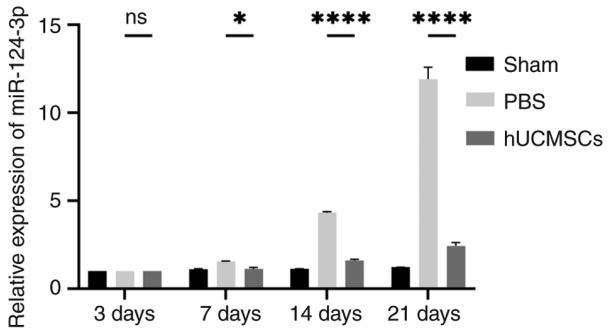

Figure 7. Comparison of miR-124 expression in spinal cord tissues of three groups of rats. miR, microRNA; ns, not significant. *P<0.05, ****P<0.0001.

that the number of BrdU$^+$/NSE$^+$ double-positive cells in the hUCMSC group was markedly higher than that in the control group, suggesting that more proliferating cells were differentiating into neurons. This implied that hUCMSCs may play a role in neural repair by promoting neuronal regeneration. The expression of the neurorepair-related protein BDNF was markedly higher in the hUCMSC group than in the control group, indicating that hUCMSCs may enhance neuronal survival and regeneration by promoting BDNF expression. Furthermore, RT-qPCR results showed that miR-124-3p expression was markedly decreased in the hUCMSCs transplantation group compared with the control group at the same time points, which was closely associated with the spinal cord repair process. This finding was consistent with that of other studies (14,24), further supporting the key regulatory role of miR-124-3p in nervous system repair. The significant changes in miR-124-3p expression not only reflect the potential mechanism of hUCMSCs in injury repair but also suggested that miR-124-3p could be an effective molecular marker for monitoring SCI repair. In motor function assessments, the BBB scores and Rivlin inclined plate test results of rats in the hUCMSC group were markedly improved compared with those in the control group, particularly on days 7 and 14 post-injury, demonstrating the positive role of hUCMSCs in promoting functional recovery after SCI.

Existing research shows that hUCMSCs have certain therapeutic effects on SCI, such as reducing neuronal apoptosis, promoting motor function recovery and reducing demyelination (25,26). However, certain studies have raised concerns regarding the stability of these effects and the mechanisms involved. For example, systematic reviews and network

meta-analyses have indicated that, although hUCMSCs have certain therapeutic effects on SCI, their efficacy is not always markedly improved compared with other treatment strategies when compared to other types of stem cells (27). By contrast, the present study employed a multi-layered experimental design to further verify the significant effects of hUCMSCs in neuronal regeneration and functional recovery, particularly in using miR-124-3p as a biomarker for evaluating the repair process, highlighting the unique advantages of hUCMSCs. In the field of miRNA research, miR-124-3p has attracted attention for its regulatory role in the nervous system. A previous study demonstrated that miR-124-3p can exert neuroprotective effects during SCI repair by regulating the interaction between glial cells and neurons and inhibiting the activation of neurotoxic microglia and astrocytes (24). The present study further confirmed, through experimental data, the close association between the upregulation of miR-124-3p and neural repair following hUCMSCs treatment, strengthening the theoretical basis for miR-124-3p as an effective monitoring marker in SCI repair.

Despite the significant therapeutic effects of intrathecal transplantation of hUCMSCs in SCI repair demonstrated in the present study, particularly the potential of miR-124-3p as a biomarker for monitoring the repair process, several limitations remain. Although animal models are indispensable in SCI research, they cannot fully represent the pathophysiological processes in humans. hUCMSCs are derived from different individuals and their cellular characteristics and functions may exhibit heterogeneity (28). This heterogeneity may lead to inconsistencies in treatment outcomes, affecting the reproducibility of research findings. Factors such as the source of hUCMSCs, culture conditions and passage number in different experiments may result in varying therapeutic performances. Although the present study confirmed the important role of miR-124-3p in SCI repair, its mechanism of action may be more complex than revealed in the present study. miR-124-3p not only participates in neuroregeneration but may also play a role in inflammation regulation, apoptosis and other processes. However, the specific functions of miR-124-3p in different cell types and stages of repair remain unclear and require further research. The present study mainly focused on the short-term effects of hUCMSCs transplantation and the changes in miR-124-3p expression. However, the long-term efficacy and safety of hUCMSCs, particularly the potential risks of immune responses or tumor formation, lack systematic long-term follow-up data (28). This is especially important when translating hUCMSCs to clinical applications. While hUCMSCs and miR-124-3p have shown significant therapeutic potential in animal models, translating these findings to human clinical applications remains challenging. Issues such as optimizing cell transplantation, monitoring post-transplantation and effectively regulating miR-124-3p expression in patients need to be addressed further (29). In conclusion, while the present study provides new insights into the treatment of SCI, caution should be exercised when translating these findings into clinical applications. Future research should validate these results in larger-scale experiments and explore ways to overcome these limitations to achieve broader and more effective clinical applications.

In summary, the present study demonstrated that intrathecal transplantation of hUCMSCs markedly promoted the recovery of hindlimb motor function following SCI in rats. Behavioral assessments, including BBB scoring and Rivlin inclined plate tests, showed a significant improvement in motor function in the hUCMSCs-treated group compared with the control group, particularly on post-surgical days 7 and 14. Histological analysis using H&E and Nissl staining further confirmed the beneficial effects of hUCMSCs, showing enhanced neuronal preservation and reduced necrotic areas. Immunofluorescence also showed an increase in $BrdU^+/NSE^+$ cells in the hUCMSC group, indicating that hUCMSCs promoted neurogenesis by enhancing cell proliferation and differentiation. The expression of the neurotrophic factor BDNF was markedly increased following hUCMSCs transplantation, further demonstrating their role in enhancing neurorepair mechanisms. In addition, the downregulation of miR-124-3p in the hUCMSC group was associated with improved motor function recovery, suggesting that miR-124-3p could be a potential biomarker for neural repair.

Overall, the present findings indicated that hUCMSCs have significant neuroprotective and regenerative effects on SCI, primarily by promoting neuronal survival, proliferation and neurotrophic support. These results suggested that hUCMSCs have great clinical application potential in SCI treatment and monitoring miR-124-3p in response to stem cell transplantation presents a novel and promising approach. One limitation of the present study is the relatively small sample size of 36 rats, which may affect the statistical power and generalizability of the results. While this sample size is consistent with previous SCI studies and was chosen due to resource and ethical considerations, future studies with larger cohorts are planned to further validate the therapeutic efficacy of hUCMSCs and the potential of miR-124-3p as a biomarker for spinal cord injury recovery.

Acknowledgements

Not applicable.

Funding

The present study was supported by Youth Project of Natural Science Foundation of Xinjiang Uygur Autonomous Region Science and Technology Department (China) (grant no. 2021D01C339).

Availability of data and materials

The data generated in the present study are included in the figures and/or tables of this article.

Authors' contributions

HQ and YW designed the study. YZ, MiA, NM and WL performed the experiments and collected the data. WL and YW drafted the manuscript. MuA, YL and XM analyzed the experimental data. MiA and NM provided necessary help during the experiments. YW and HQ provided guidance and funding support for the study. HQ and YZ confirm the

authenticity of all the raw data. All authors read and approved the final manuscript.

Ethics approval and consent to participate

All animal experiments were approved by the Animal Ethics Committee of Xinjiang Medical University (Urumqi, China; approval no. IACUC-20230321-07). All procedures used in the animal experiments adhered to the standards of the principles of management and protection of experimental animals and the utmost care was taken to minimize the number of animals used and their suffering.

Patient consent for publication

Not applicable.

Competing interests

The authors declare that they have no competing interests.

References

1. Hu X, Xu W, Ren Y, Wang Z, He X, Huang R, Ma B, Zhao J, Zhu R and Cheng L: Spinal cord injury: Molecular mechanisms and therapeutic interventions. Signal Transduct Target Ther 8: 245, 2023.
2. Sterner RC and Sterner RM: Immune response following traumatic spinal cord injury: Pathophysiology and therapies. Front Immunol 13: 1084101, 2022.
3. Eli I, Lerner DP and Ghogawala Z: Acute traumatic spinal cord Injury. Neurol Clin 39: 471-488, 2021.
4. Wang LT, Liu KJ, Sytwu HK, Yen ML and Yen BL: Advances in mesenchymal stem cell therapy for immune and inflammatory diseases: Use of cell-free products and human pluripotent stem cell-derived mesenchymal stem cells. Stem Cells Transl Med 10: 1288-1303, 2021.
5. Li K, Yan G, Huang H, Zheng M, Ma K, Cui X, Lu D, Zheng L, Zhu B, Cheng J and Zhao J: Anti-inflammatory and immunomodulatory effects of the extracellular vesicles derived from human umbilical cord mesenchymal stem cells on osteoarthritis via M2 macrophages. J Nanobiotechnology 20: 38, 2022.
6. Zhou X, Liu X, Liu L, Han C, Xie Z, Liu X, Xu Y, Li F, Bi J and Zheng C: Transplantation of IFN-γ Primed hUCMSCs significantly improved outcomes of experimental autoimmune encephalomyelitis in a mouse model. Neurochem Res 45: 1510-1517, 2020.
7. Wei P, Jia M, Kong X, Lyu W, Feng H, Sun X, Li J and Yang JJ: Human umbilical cord-derived mesenchymal stem cells ameliorate perioperative neurocognitive disorder by inhibiting inflammatory responses and activating BDNF/TrkB/CREB signaling pathway in aged mice. Stem Cell Res Ther 14: 263, 2023.
8. Huang J, U KP, Yang F, Ji Z, Lin J, Weng Z, Tsang LL, Merson TD, Ruan YC, Wan C, *et al*: Human pluripotent stem cell-derived ectomesenchymal stromal cells promote more robust functional recovery than umbilical cord-derived mesenchymal stromal cells after hypoxic-ischaemic brain damage. Theranostics 12: 143-166, 2022.
9. Wei Z, Hang S, Wiredu Ocansey DK, Zhang Z, Wang B, Zhang X and Mao F: Human umbilical cord mesenchymal stem cells derived exosome shuttling mir-129-5p attenuates inflammatory bowel disease by inhibiting ferroptosis. J Nanobiotechnology 21: 188, 2023.
10. Zhao H, Li Y, Chen L, Shen C, Xiao Z, Xu R, Wang J and Luo Y: HucMSCs-Derived miR-206-knockdown exosomes contribute to neuroprotection in subarachnoid hemorrhage induced early brain injury by targeting BDNF. Neuroscience 417: 11-23, 2019.
11. Mavroudis I, Balmus IM, Ciobica A, Nicoara MN, Luca AC and Palade DO: The role of microglial exosomes and miR-124-3p in neuroinflammation and neuronal repair after traumatic brain injury. Life (Basel) 13: 1924, 2023.
12. Yan Q, Sun SY, Yuan S, Wang XQ and Zhang ZC: Inhibition of microRNA-9-5p and microRNA-128-3p can inhibit ischemic stroke-related cell death in vitro and in vivo. IUBMB Life 72: 2382-2390, 2020.
13. Cheng Z, Li X, Ye X, Yu R and Deng Y: Purpurogallin reverses neuronal apoptosis and enhances 'M2' polarization of microglia under ischemia via mediating the miR-124-3p/TRAF6/NF-κB axis. Neurochem Res 48: 375-392, 2023.
14. Li R, Zhao K, Ruan Q, Meng C and Yin F: Bone marrow mesenchymal stem cell-derived exosomal microRNA-124-3p attenuates neurological damage in spinal cord ischemia-reperfusion injury by downregulating Ern1 and promoting M2 macrophage polarization. Arthritis Res Ther 22: 75, 2020.
15. Ge X, Guo M, Hu T, Li W, Huang S, Yin Z, Li Y, Chen F, Zhu L, Kang C, *et al*: Increased microglial exosomal miR-124-3p alleviates neurodegeneration and improves cognitive outcome after rmTBI. Mol Ther 28: 503-522, 2020.
16. National Research Council (US) Committee for the Update of the Guide for the Care and Use of Laboratory Animals: Guide for the Care and Use of Laboratory Animals. 8th edition. National Academies Press (US), Washington, DC, 2011.
17. Chen JN, Zhang YN, Tian LG, Zhang Y, Li XY and Ning B: Down-regulating circular RNA Prkcsh suppresses the inflammatory response after spinal cord injury. Neural Regen Res 17: 144-151, 2022.
18. Basso DM, Beattie MS and Bresnahan JC: A sensitive and reliable locomotor rating scale for open field testing in rats. J Neurotrauma 12: 1-21, 1995.
19. Wang X, Hong CG, Duan R, Pang ZL, Zhang MN, Xie H and Liu ZZ: Transplantation of olfactory mucosa mesenchymal stromal cells repairs spinal cord injury by inducing microglial polarization. Spinal Cord 62: 429-439, 2024.
20. Livak KJ and Schmittgen TD: Analysis of relative gene expression data using real-time quantitative PCR and the 2(-Delta Delta C(T)) Method. Methods 25: 402-408, 2001.
21. Huang Y, Wu Q and Tam PKH: Immunomodulatory mechanisms of mesenchymal stem cells and their potential clinical applications. Int J Mol Sci 23: 10023, 2022.
22. Zhou H, Shen X, Yan C, Xiong W, Ma Z, Tan Z, Wang J, Li Y, Liu J, Duan A and Liu F: Extracellular vesicles derived from human umbilical cord mesenchymal stem cells alleviate osteoarthritis of the knee in mice model by interacting with METTL3 to reduce m6A of NLRP3 in macrophage. Stem Cell Res Ther 13: 322, 2022.
23. Toader C, Dobrin N, Brehar FM, Popa C, Covache-Busuioc RA, Glavan LA, Costin HP, Bratu BG, Corlatescu AD, Popa AA and Ciurea AV: From recognition to remedy: The significance of biomarkers in neurodegenerative disease pathology. Int J Mol Sci 24: 16119, 2023.
24. Jiang D, Gong F, Ge X, Lv C, Huang C, Feng S, Zhou Z, Rong Y, Wang J, Ji C, *et al*: Neuron-derived exosomes-transmitted miR-124-3p protect traumatically injured spinal cord by suppressing the activation of neurotoxic microglia and astrocytes. J Nanobiotechnology 18: 105, 2020.
25. Wang S, Jia Y, Cao X, Feng S, Na L, Dong H, Gao J and Zhang L: HUCMSCs transplantation combined with ultrashort wave therapy attenuates neuroinflammation in spinal cord injury through NUR77/NF-κB pathway. Life Sci 267: 118958, 2021.
26. Liao Z, Yang X, Wang W, Deng W, Zhang Y, Song A, Ni B, Zhao H, Zhang S and Li Z: hucMSCs transplantation promotes locomotor function recovery, reduces apoptosis and inhibits demyelination after SCI in rats. Neuropeptides 86: 102125, 2021.
27. Liu S, Zhang H, Wang H, Huang J, Yang Y, Li G, Yu K and Yang L: A comparative study of different stem cell transplantation for spinal cord injury: A systematic review and network meta-analysis. World Neurosurg 159: e232-e243, 2022.
28. Akhlaghpasand M, Tavanaei R, Hosseinpoor M, Yazdani KO, Soleimani A, Zoshk MY, Soleimani M, Chamanara M, Ghorbani M, Deylami M, *et al*: Safety and potential effects of intrathecal injection of allogeneic human umbilical cord mesenchymal stem cell-derived exosomes in complete subacute spinal cord injury: A first-in-human, single-arm, open-label, phase I clinical trial. Stem Cell Res Ther 15: 264, 2024.
29. Subbarayan R, Murugan Girija D, Raja STK, Krishnamoorthy A, Srinivasan D, Shrestha R, Srivastava N and Ranga Rao S: Conditioned medium-enriched umbilical cord mesenchymal stem cells: A potential therapeutic strategy for spinal cord injury, unveiling transcriptomic and secretomic insights. Mol Biol Rep 51: 570, 2024.